Tetrameric Assembly of Full-Sequence Protein Zero Myelin Glycoprotein by Synchrotron X-Ray Scattering

Hideyo Inouye,* Hiro Tsuruta,# Jan Sedzik,§ Keiichi Uyemura,§ and Daniel A. Kirschner*

*Department of Biology, Boston College, Chestnut Hill, Massachusetts 02467 USA; #Stanford Synchrotron Radiation Laboratory/Stanford Linear Accelerator Center, Stanford University, Stanford, California 94309-0210; and §Department of Physiology, Keio University School of Medicine, Shinanomachi, Shinjuku-ku, Tokyo 160, Japan

ABSTRACT Highly purified myelin P0 glycoprotein was solubilized to 1–8 mg/ml in 0.1% sodium dodecyl sulfate (SDS), and the solution structure of the P0 assembly was studied using synchrotron x-ray scattering. The full-length P0, which was isolated from bovine intradural roots, included both the extracellular and cytoplasmic domains of the molecule. At the higher concentrations (4, 6, and 8 mg/ml, respectively), an x-ray intensity maximum was observed at 316 Å, 245 Å, and 240 Å Bragg spacing. Because the position of this intensity depended on P0 concentration, it is most likely due to interparticle interference. By contrast, the position of a second intensity maximum, which was at ~40 Å Bragg spacing, was invariant with P0 concentration. This latter intensity was accounted for by monodispersed, 80 Å-diameter particles that are composed of eight, ~30 Å-diameter spheres. Chemical parameters suggest that the 80 Å particles correspond to the size of a tetramer of P0 molecules. Therefore, the ~30 Å spheres would correspond to the sizes of the extracellular and cytoplasmic domains for each of the P0 monomers. The invariance of the second intensity maximum with P0 concentration indicates that the structure of the 80 Å-diameter, tetrameric particles is unaltered. According to the liquid model for interparticle interference from charged spheres, the 80 Å-diameter particle has 10 negative surface charges which likely arise from negatively charged SDS molecules bound to the transmembrane domain of P0. This binding, however, apparently does not alter the tetrameric assembly of P0, suggesting that intermolecular interactions involving extracellular domains and cytoplasmic domains likely stabilize this assembly. Some of our results have been published in abstract form (Inouye, H., H. Tsuruta, D. A. Kirschner, J. Sedzik, and K. Uyemura. Abstracts of the 4th International School and Symposium on Synchrotron Radiation in Natural Science, June 15–20, 1998. Ustron-Jaszowiec, Poland. p. 31).

INTRODUCTION

Protein zero (P0) is the major integral protein of myelin in the peripheral nervous system across a wide phylogenetic range that includes amphibian, avian, reptilian, and mammalian species (Uyemura et al., 1992). In fish, P0 is the major protein in both CNS and PNS myelins (Kirschner et al., 1989; Inouye and Kirschner, 1991). The atomic structure for the hydrophilic, extracellular domain of P0 was determined by x-ray crystallography (Shapiro et al., 1996). The crystal lattice is body-centered (space group I422), and the lattice constants are $a = b = 88.9$ Å and $c = 91.6$ Å. The asymmetric unit in the unit cell is a single molecule that is similar to immunoglobulin V_H domains, as previously predicted by us (Inouye and Kirschner, 1991; Wells et al., 1993; Kirschner et al., 1996). Three different molecular interfaces are evident in the crystal: the first is between the protomers that are related by a fourfold symmetry axis, the second is between oppositely directed molecules (from different tetramers) that are related by a twofold axis normal to the fourfold axis, and the third is at the head-to-head interaction between monomers of the packed tetramers in the crystal. The number density of P0 extracellular domains in the crystal is consistent with that evaluated from the chemical composition of isolated myelin membranes (Inouye and Kirschner, 1988b), suggesting that there is a network of P0 tetramers in the myelin (Shapiro et al., 1996).

Whether the proposed tetrameric assembly of P0 molecules actually exists in intact myelin is not yet established. Analytical ultracentrifugation suggests that the tetrameric assembly of P0 extracellular domains in solution is energetically favored (Shapiro et al., 1996); however, the solution behavior of the *complete* P0 molecule, which includes *both* the extracellular and cytoplasmic domains, has not yet been studied. In the present report we have isolated the complete P0 molecule from bovine intradural root myelin, solubilized it in 0.1% (3.47 mM) sodium dodecyl sulfate (SDS) in water, and analyzed the solution x-ray scattering for different protein concentrations ranging from 1 to 8 mg/ml. In our experiments, SDS alone in the absence of salt does not form micelles, and therefore is a valid lipid bilayer mimetic for the transmembrane P0 protein. We show here that full-sequence P0 molecules form a tetrameric assembly in solution. Comparison among the electron density profiles for the P0-SDS complex, SDS micelles, and nerve myelin membranes is used to localize P0 in myelin.

Received for publication 9 February 1998 and in final form 17 September 1998.

Address reprint requests to Drs. Hideyo Inouye and D. A. Kirschner, Department of Biology, Boston College–Higgins Hall, 140 Commonwealth Avenue, Chestnut Hill, MA 02467-3811. Tel.: 617-552-0213; Fax: 617-552-2011; E-mail: inouye@amy.bc.edu; kirschnd@bc.edu.

J. Sedzik's current addresses are Uppsala University, Department of Medical Genetics and Pathology, Department of Biochemistry, 751-23 Uppsala, Sweden and National Institute of Bioscience and Human-Technology, 1-1-4 Higashi, Tsukuba, Ibaraki 305-8566, Japan.

0006-3495/99/01/423/15 $2.00

MATERIALS AND METHODS

Purification and concentration of bovine P0 protein

Intradural bovine spinal roots and spinal cord were purchased from a local slaughterhouse (Tokyo, Japan) and transported on ice to the laboratory (Keio University, Tokyo). Myelin membranes were purified according to conventional methods (Norton, 1974). P0 glycoprotein was purified as described in Sedzik et al. (1998a; J. Sedzik, Y. Kotake, and K. Uyemura, submitted for publication). Briefly, the purified myelin was dispersed by motor-driven homogenization in 50 ml 2% SDS in 50 mM Tris-HCl pH 7.4–8.4, and incubated overnight in the cold (4°C). The cloudy dispersion was filtered at room temperature through Qualitative Filter Paper Number 2 (Toyo Roshi Kaisha, Ltd., Tokyo, Japan). The filtered extract was then diluted fivefold (to 250 ml) with buffer (50 mM Tris-HCl), and NaCl was added to a final salt concentration of 0.5 M. A Cu^{2+}-immobilized metal affinity chromatography column (1 cm × 30 cm) was prepared according to the manufacturer's instructions (Pharmacia Biotech, Sweden). The total extract of PNS myelin protein was applied at a flow rate maintained at 0.5–1 ml/min, and 1–2.5-ml fractions were collected (corresponding to 100–250 drops; paper speed 1 mm/ml). After application of the protein extract, the IMAC column was washed extensively in starting buffer containing 0.1% SDS with a high salt content. When the baseline stabilized, a volume of starting buffer corresponding to threefold the column volume was applied but without salt to elute a crude P0 fraction. The pooled P0 fractions were applied to a ConA-Agarose column (1 cm × 20 cm) prepared according to the manufacturer's instructions; and the eluant was a 0.0–0.1 M gradient of methyl-D-mannose. The collected P0 samples were applied to the PD-10 column, and an eluant of 0.1% SDS in water was used to remove salt and mannose. The content of P0 was determined by Lowry assay. The amount of residual phospholipid was kindly measured by Dr. Y. Kotake using the method of Bartlett (1959) or a commercially available phospholipid test kit (Wako Pure Chemical Industries, Ltd., Japan) based on the Hoeflmayr-Fried method (Hoeflmayr and Fried, 1966). In brief, after precipitation by 5% TCA, phospholipids and protein were digested with sulfuric acid and permanganate salts in boiling water. Liberated inorganic phosphate was measured after addition of ammonium molybdate and reductant.

The aqueous solution of P0 in 0.1% SDS was concentrated up to 100 mg/ml without detectable precipitation using a B15 Minicon Concentrator (Amicon, Bedford, MA). The color of the concentrated P0 in 0.1% SDS was deep yellow. The N-terminal amino acid sequence of the purified P0 was determined using Protein Sequencing System Model 473A (Perkin-Elmer, Applied Biosystem, Foster City, CA) according to the manufacturer's instructions. The samples applied for amino acid analysis were either the concentrated solution of P0 protein dialyzed against 0.1% SDS in water, or a strip of the polyvinylidene difluoride Imobilon transfer membranes stained by Coomassie Brilliant Blue R-250 to indicate the position of P0. The full analysis of the first 10 amino acids usually was done as an overnight run and was as previously described (Sakamoto et al., 1987). The protein purification procedure has been reported in abstract form (Sedzik et al., 1997),

Synchrotron x-ray scattering

Sample

The stock solution for the x-ray experiments was 20 mg/ml P0 in 0.1% SDS. The solution was diluted by 0.1% SDS to prepare 1, 2, 4, 6, and 8 mg/ml solutions. The 0.1% SDS solution without P0 was examined as a control.

X-ray scattering

All solution scattering measurements were conducted at Beam Line 4-2, the Stanford Synchrotron Radiation Laboratory, using the improved version of the Biotechnology Research Resource small-angle scattering/diffraction instrument (Wakatsuki et al., 1992). The synchrotron beam from an 8-pole wiggler was focused with a bent cylinder mirror and monochromatized with a double-crystal Si(111) monochromator. The beam energy was calibrated to 8979 eV (1.381 Å) using the CuKα absorption edge. The x-ray beam, ~2.5 mm (horizontal) × 0.8 mm (vertical) measured as full-width at half-maximum, FWHM), irradiated a solution sample cell equipped with synthetic mica windows. The x-ray path length of the cell was 1.6 mm. A one-dimensional gas proportional counter (BioLogic 210, Grenoble, France) was placed 2.31 m downstream from the sample position, covering the range of Bragg spacing 26–780 Å. The direct beam position was found by measuring the (100) reflection from a cholesterol myristate powder sample. The sample-to-detector distance was measured using the (100) reflection position with a known detector channel width. Solution x-ray scattering was measured every 1–2 min with total exposure time per sample solution of 10–15 min. The incident beam intensity was measured during the course of measurement with a short-path ionization chamber placed immediately upstream of the sample cell. The detector count rate ranged from 12,000 to 20,000 counts/s, a range approximately one order of magnitude below the high count rate limit of the detector system. Individual scattering curves were immediately inspected for potential radiation-induced aggregation, and none of the curves indicated any such effect.

Data reduction of solution scattering

The protein solution scattering curves were scaled to one another according to the integrated intensity of the direct beam. The scattering contribution of instrumental background (primarily vacuum window scattering), the empty cell (mica windows), and the buffer solution were subtracted from each protein scattering curve. The scattering intensity from 0.1% SDS in water was negligible compared to that from the protein solution. No absorption correction was made since the difference in the x-ray beam flux absorbed by the protein solution samples and the buffer solution alone was <1% for the range of protein concentrations we employed.

Absolute electron density profile of nerve myelin membrane

Specimens

Freshly dissected sciatic nerves of mouse were sealed into thin-wall capillary tubes containing saline at low ionic strength (0.06) and at pH 6.0 (Inouye and Kirschner, 1988a). To fix the electron density of the fluid we used hypotonic saline containing 10% glycerol solution with buffer. The electron density of 60 mM NaCl is 0.3347 and of 10% glycerol is 0.3474 e/Å^3.

X-ray diffraction

Diffraction experiments were carried out using nickel-filtered and either single- or double-mirror focused CuKα radiation from a Rigaku X-ray generator (40 kV, 20 mA) or from an Elliott GX-20 rotating-anode generator (35 kV, 40 mA; 200 μm focal spot). The diffraction patterns were recorded with Kodak No-Screen or Direct Exposure X-ray films. The absorbances of the films were determined on an Optronics Photoscan P-1000 microdensitometer (Optronics International, Inc., Chelmsford, MA) using a 25-μm raster.

Calculation of absolute density

The structure factors were measured at reciprocal coordinate $R = h/d$, where h is an integer and d is the myelin period for two different fluid electron densities f_1 and f_2 in the extracellular space. The observed structure factors are then related by

$$K_1F_{1\text{obs}}(h/d) - K_2F_{2\text{obs}}(h/d) = w_0\text{sinc}(\pi w_0 h/d)(f_2 - f_1),$$

where w_0 is the thickness of a pair of membrane excluded from the medium, and K_1 and K_2 are scaling factors of the observed structure factors F_{1obs} and F_{2obs}. Given a constant period $d = 216$ Å, and media densities $f_1 = 0.3347$ e/Å^3 and $f_2 = 0.3474$ e/Å^3, the scaling factors K_1, K_2, and w_0 were obtained using the six observed orders of reflection. The best scaling factors were obtained when the residual R (the difference between the left and right terms) was a minimum. We averaged three sets of diffraction patterns having identical 216 Å-periods for media f_1 and f_2, respectively. The observed structure factors F(1)–F(6) (with mean errors in parentheses) for the media f_1 and f_2 were, respectively: 0.0, 0.40 (0.03), 1.74 (0.05), 0.43 (0.18), −1.41 (0.04), −1.02 (0.04); and −0.14 (.01), 0.56 (.03), 1.80 (0.05), 0.36 (0.04), −1.35 (0.02), −0.97 (0.04). We found the exclusion length $w_0 = 136$ Å, and the scale factors $K_1 = K_2 = 2$ at the minimum $R = 42.5\%$.

Physical-chemical analysis of amino acid sequence of P0 protein

The sequence of bovine P0-glycoprotein is known (Sakamoto et al., 1987). The physicochemical characterizations from the sequence (i.e., hydrophobicity, secondary structure propensity, pH titration, molecular weight) were determined according to Inouye and Kirschner (1991).

RESULTS AND INTERPRETATION

Solution x-ray scattering from P0 in dilute SDS

The x-ray scattering curves as a function of the reciprocal coordinate (2 sin θ/λ, where 2θ is the scattering angle and λ is x-ray wavelength) was measured for different P0 concentrations, ranging from 1 to 8 mg/ml in 0.1% SDS. At 1 and 2 mg/ml (Fig. 1), the scattering intensity decreased monotonically to ~0.014 Å^{-1}, while at the higher concentrations an intensity maximum was observed at ~0.003–0.004 Å^{-1} (Fig. 2). The reciprocal coordinate of the peak in this range shifted to higher values with increasing concentration. At reciprocal coordinates >~0.01 Å^{-1} the intensity curves (on a relative scale) were similar for different concentrations, showing a broad intensity maximum at ~0.022 Å^{-1} and with neighboring intensity minima at ~0.015 Å^{-1} and ~0.03 Å^{-1}. That the position of the intensity maximum at ~0.003–0.004 Å^{-1} depended on protein concentration indicates that this small-angle peak arises from interparticle interference. The invariance of the position of the second peak and its distinct neighboring intensity minima indicate that this peak arises from the Fourier transform of nearly spherically symmetric particles, and that the particle size remains constant over the concentration range.

Correlation functions were calculated from the observed scattering curves for P0 concentrations of 1 and 2 mg/ml (Fig. 3, *lower curves*) and for 4 and 8 mg/ml (Fig. 3, *upper curves*) according to Eq. 6 (Appendix). The curves were similar for all the intensity data, showing a minimum at ~30 Å, a maximum at ~43 Å, and a zero value at ~80 Å. The latter value indicates the exclusion length. The peak at ~43 Å is interpreted as the interference between the subunits within the 80 Å-diameter particle, and the minimum at ~30 Å refers to the diameter of the subunit. The interparticle interference is not present in the scattering data for P0 concentrations at 1 and 2 mg/ml. Assuming spherical symmetry for the particle, the phases are either 0 or π, and these alternate at the intensity minima. Since F(0) should be positive, the phase of the first loop is set to zero. The intensity minimum occurs at 1.4877×10^{-2} Å^{-1} for 2 mg/ml. The radial projection of the electron density of the particle was calculated according to Eq. 1 (see Appendix), and shows a double shell structure where the electron density is low at the center and high at the periphery (Fig. 4, *thick line*). The electron density becomes that of the medium at $r \approx 40$ Å, which agrees with the exclusion length derived from the correlation function. The calculated intensity from this radial projection of the electron density distribution (Fig. 5) fits the scattering curve recorded for P0 at 2 mg/ml with a residual $R = 7.7\%$.

At higher P0 concentration (e.g., Fig. 2) the interparticle interference is observed at Bragg spacings of 316 Å, 245 Å, and 240 Å for 4, 6, and 8 mg/ml P0, respectively. According

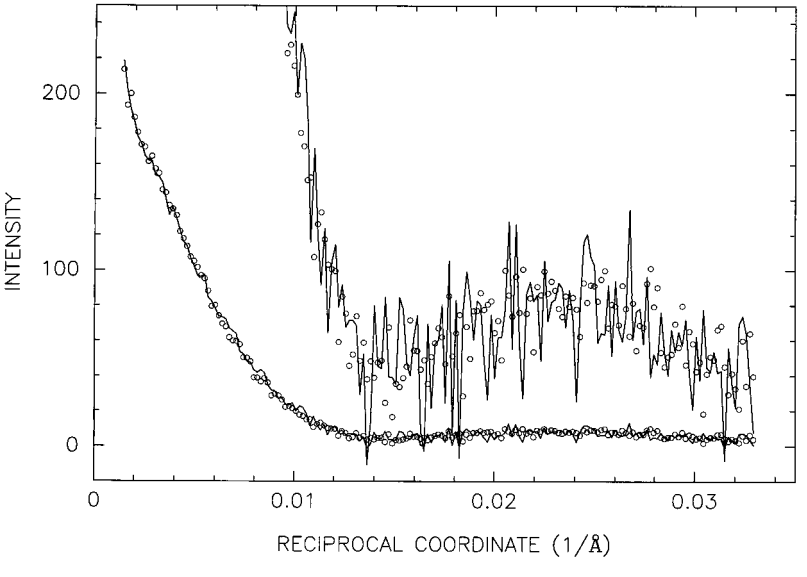

FIGURE 1 Synchrotron x-ray scattering for P0 solution (1 mg/ml, *solid line*; 2 mg/ml, *circles*) in 0.1% sodium dodecyl sulfate (SDS) at pH 7.4. Scattering intensity is plotted as a function of reciprocal coordinate (2 sin θ/λ, where 2θ is the scattering angle and λ is x-ray wavelength). The curves are normalized so that the area under each is unity. The upper two curves are on a 10-fold expanded intensity scale.

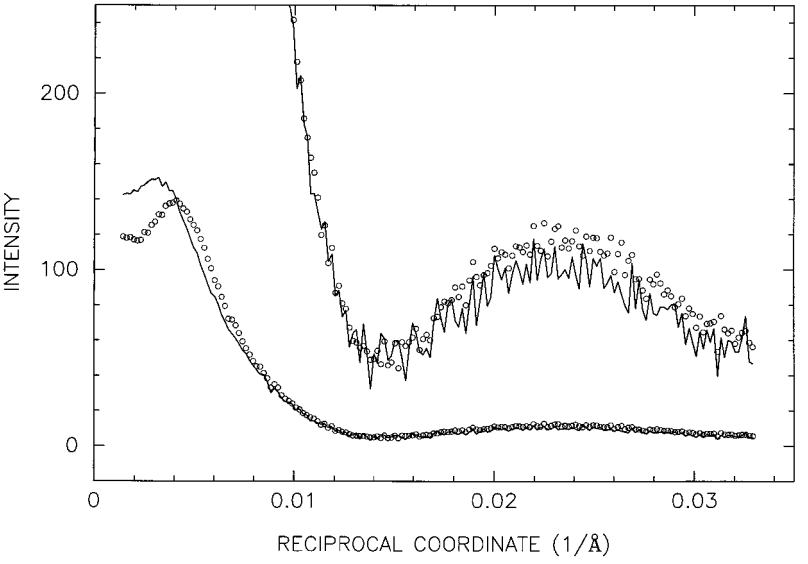

FIGURE 2 Synchrotron x-ray scattering for P0 solution (4 mg/ml, *solid line*; 8 mg/ml, *circles*) in 0.1% SDS at pH 7.4. Scattering intensity is plotted as a function of reciprocal coordinate (2 sin θ/λ, where 2θ is the scattering angle and λ is x-ray wavelength). The curves are normalized so that the area under each is unity. The upper two curves are on a 10-fold expanded intensity scale.

to Ehrenfest (Guinier, 1963) the interference term in Eqs. 3 and 5 can be expressed as $1 + \sin(2\pi aR)/(2\pi aR)$ where a is the interparticle distance. The interference maximum occurs at reciprocal coordinate R where $aR = 1.23$. This equation gives peak positions similar to the observed ones (not shown), and the interparticle distances are calculated to be 388 Å, 301 Å, and 295 Å, respectively (Table 1).

Chemical interpretation

Comparison with structures of SDS micelle and myelin membrane

The current study using x-ray scattering indicates that solutions of P0 solubilized in 0.1% SDS contain spherical, 80 Å-diameter particles that have a low electron density at their core and high electron density at their periphery. Such a double shell structure is similar to that for micellar SDS (Reiss-Husson and Luzzati, 1964, 1966). In an x-ray study of SDS micelles, Kratky and Müller (1982) derived the electron density levels for a double shell model having parameters $r_i = 16$ Å, $r_o = 32$ Å, $\rho_i = 0.285$ e/Å^3, $\rho_o = 0.36$ e/Å^3, and $\rho_s = 0.33$ e/Å^3, where r_i and r_o are the inner and outer radii, ρ_i and ρ_o are the inner and outer electron density, and ρ_s is the solvent electron density (see Eq. 2 in Appendix). The micellar mass is 23 kDa, the apparent partial specific volume is 0.875 cm^3/g, and the aggregation number is 80 (Kratky and Müller, 1982). Given this aggregation number, the SDS molecules cannot pack into spheres, which means the micelle must be slightly nonspherical (Israelachvili, 1992). Assuming a spherical, 16 Å-radius SDS micelle has a core electron density of 0.285 e/Å^3 and 97 electrons/SDS hydrocarbon chain, the aggregation number is calculated to be ~50, which is similar to the value given by Israelachvili (1992).

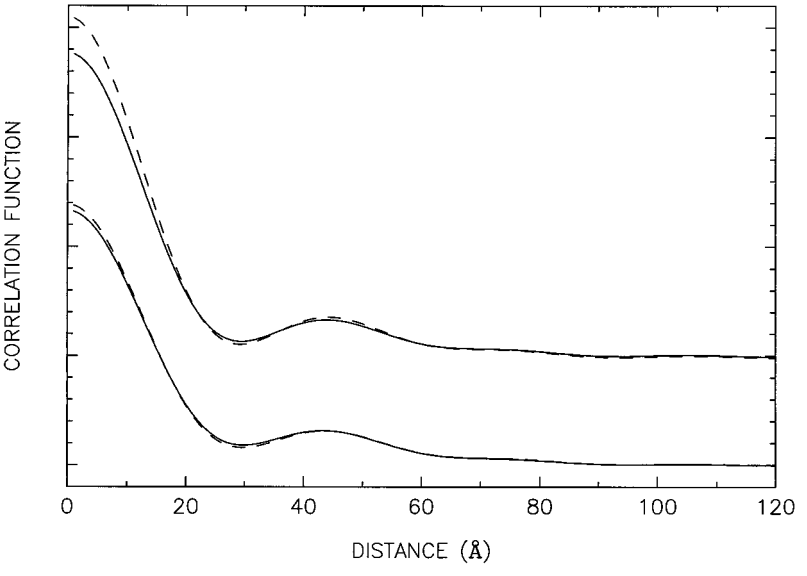

FIGURE 3 The correlation functions calculated from the observed scattering intensities for different P0 concentrations. *Lower curves:* 1 mg/ml (*solid line*) and 2 mg/ml (*dashed line*); *Upper curves:* 4 mg/ml (*solid line*) and 8 mg/ml (*dashed line*). The baselines of the lower curves are offset by five units.

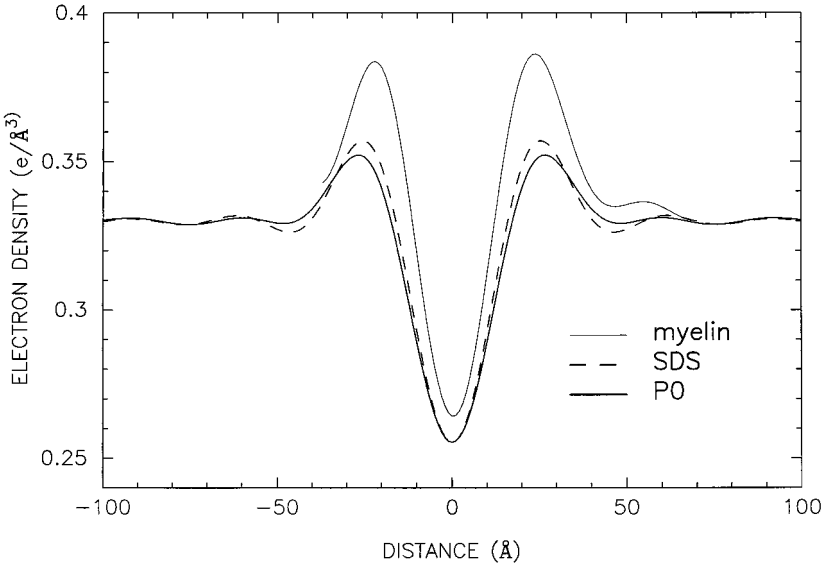

FIGURE 4 The radial electron density profiles on an absolute scale for 2 mg/ml P0 in 0.1% SDS (*heavy solid line*), mouse sciatic nerve (*thinner solid line*), and SDS micelle (*dashed line*). For the P0 sample, the amplitude was derived from the observed scattering intensity (Fig. 1) assuming that the phase of the first loop is 0 radian and the second loop is π. The absolute scale was determined assuming that the electron density levels at the core of the particle and in the fluid are the same as the corresponding ones for SDS micelles. For the SDS micelle, the amplitude was first calculated from the step-function model (Kratky and Müller, 1982) in the same reciprocal coordinate range as for the observed scattering intensity, then the electron density on an absolute scale was calculated. Note such a truncation of the intensity data broadens the initial step function. For the mouse sciatic nerve, the tissue was dissected out and immediately sealed into thin-wall capillary tubes containing hypotonic medium at pH 6.0 and ionic strength 0.06. The absolute scale was determined by comparing the diffraction patterns having myelin periods of 216 Å for 1–6 orders but with different electron density levels of fluid, i.e., 0.3347 e/Å^3 and 0.3474 e/Å^3 for 60 mM NaCl hypotonic buffer (Inouye and Kirschner, 1988a) and buffer containing 10% glycerol, respectively. The calculated average electron density was 0.343 e/Å^3, which is similar to the ones from frog sciatic nerve, 0.343 e/Å^3 (Worthington and Blaurock, 1969) and 0.347 e/Å^3 (Blaurock, 1971). Note that the electron density peaks of the P0 solution are further apart than those of the myelin membrane and of the SDS micelle, indicating the positions of the extracellular and cytoplasmic domains of the P0 molecule.

By using these step-function parameters, we calculated the spherically averaged intensity in the same reciprocal range as the experimental data (Fig. 5). The SDS scattering intensity at low angle is weaker and the one at wider angle is higher than that observed for P0 in SDS (Figs. 1, 2, and 5). This difference arises from the thickness of the wall of the spherical particle. The electron density profile on an absolute scale for an SDS micelle is calculated from this intensity curve in the observed range of the reciprocal coordinate. As expected from the above intensity distribution, the SDS micelle gives a narrower polar headgroup than the P0-SDS system (Fig. 4, *dashed curve*). This indicates that the extracellular and cytoplasmic domains of the P0 molecule are located beyond the polar headgroups of the SDS molecules (cf. *dashed* and *thicker solid curves* of Fig. 4). The absolute electron density profile for mouse sciatic nerve (Fig. 4, *thin solid curve*) is similar to the one previously reported for frog sciatic nerve (Worthington and Blaurock, 1969; Blaurock, 1971). The highest electron density peaks in myelin correspond to the polar headgroup layers of polar lipids, and the extracellular and cytoplasmic domains of P0 are apparently located just outside of these peaks.

Stoichiometry of the chemical components

To interpret the x-ray model in terms of chemical constituents, we must determine the stoichiometry. Consider a spherical particle of radius r_o, which is composed of protein, SDS, and water. Here the lipid content is negligible, as the molar ratio of phosphorus and P0 protein is measured as 1:70 (Sedzik et al., 1998a; J. Sedzik, Y. Kotake, and K. Uyemura, submitted for publication). The interparticle space is assumed to be entirely composed of water. When the particles are monodispersed in solution, and the distance between them is a, the volume occupied by one particle is V, and the particle volume is $v = 4\pi r_o^3/3$, where $r_o = 40$ Å. The occupied volume V is given by $0.71a^3$ from the volume fraction of a face-centered cubic lattice (Guinier and Fournet, 1955). The numbers of components in the particle are derived according to Eqs. 20 and 21 (Appendix). The interparticle interference peak was observed only for the P0 concentration at 4, 6, and 8 mg/ml. The number of P0 molecules per particle is calculated to be either three or four for 6 mg/ml and four for 4 and 8 mg/ml (see Table 1). Since the interference peak at $\sim$0.003–0.004 Å^{-1} was not observed for P0 concentrations of 1 and 2 mg/ml, the number of P0 molecules was not calculated, but assumed to be four.

Surface charge of 80 Å particle

For spherically symmetric monodispersed particles, the intensity function is given by two terms (Eq. 7 in Appendix): $F(R)^2$, the particle structure factor; and $S(R)$, the interparticle interference. Here the particle structure factor was given

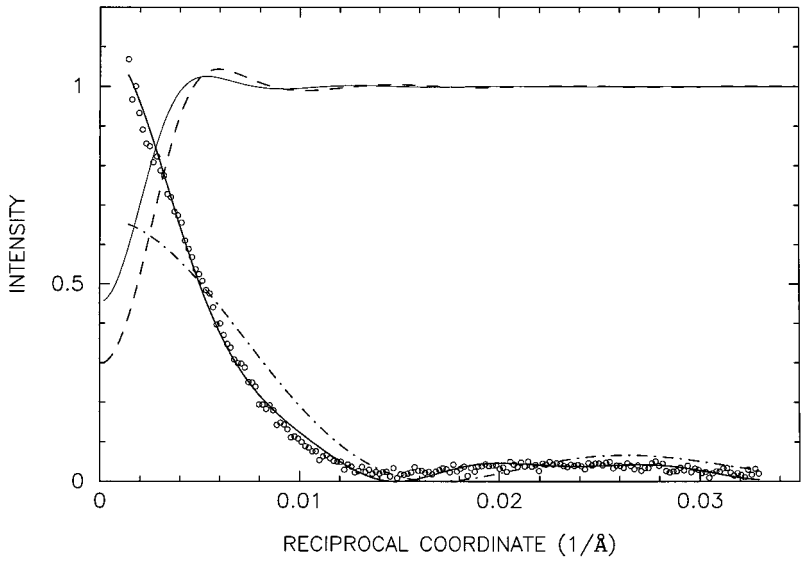

FIGURE 5 Scattering intensity plotted as a function of reciprocal coordinate (2 sin θ/λ, where 2θ is the scattering angle and λ is x-ray wavelength). *Lower curves:* The observed (*circles*) and calculated normalized scattering intensities for 2 mg/ml P0 in 0.1% SDS (*solid line*) and for SDS micelle (*dashes and dots*). The latter includes that calculated from the electron density profile of the P0 solution (Fig. 4, *thicker line*) and from the profile of the SDS micelle (Fig. 4, *dashes*). While the difference in the electron density profiles between the P0 solution and the SDS micelle appears to be minimal in Fig. 4, the difference in the calculated intensity between them is obvious here. (The structure factors are multiplied by 0.005.) *Upper curves:* Hayter-Penfold structure factors (interference term). The surface charge was optimized against the observed solution scattering from P0 (4 mg/ml, *solid line*; 8 mg/ml, *dashed line*). The given parameters include diameter of the sphere (80 Å), ionic strength (1.7×10^{-3}), temperature (25°C), dielectric constant (78.3), and number of P0 molecules per particle (4). The volume fractions were 6.5×10^{-3} and 1.3×10^{-2}, and the effective diameters were 126 Å and 109 Å for 4 and 8 mg/ml, respectively. The number of surface charges for both solutions was 10 (30 mV).

by the calculated intensity from the electron density profile for the 2 mg/ml P0 sample (Fig. 5, *lower solid line*), because the scattering at this concentration showed no interference peak. The interparticle interference term was calculated according to liquid theory (see Appendix) with input parameters of temperature, ionic strength, particle size, total volume available for a particle (inverse to the number density), and surface charge (or potential). Of these parameters, temperature, ionic strength, and number density are known from the experimental conditions. The aggregation number for P0 was chosen to be 4 for P0 concentrations of 4 and 8 mg/ml, and the particle size was set to be 80 Å from the evidence of the particle structure factor as discussed above. It was assumed that Na^+ ions of SDS molecules are fully dissociated and the negatively charged moiety of the SDS molecules is bound to P0. Then, the ionic strength was

TABLE 1 Stoichiometry of SDS-P0 particle

c* (mg/ml)	d_{obs}# (Å)	a§ (Å)	N_{P0}¶	N_{SDS}‖	$N_{water\text{-}in}$**	Mass## (kDa)	Density§§ (g/ml)	g_{SDS}/g_{P0}
1	—	614‖‖	4‖‖	344	29	198	1.23	1.00
2	—	487‖‖	4‖‖	171	2477	193	1.19	0.498
4	315.7	388	4	87	3631	190	1.18	0.253
6	244.8	301	3	40	5517	181	1.12	0.155
8	240.0	295	4	38	4816	185	1.15	0.110

The concentration of SDS was constant at 0.1% (3.47 mM).
*c, P0 concentration, corresponding in mM to 0.04, 0.08, 0.16, 0.24, and 0.32.
#d_{obs}, Bragg spacing of the observed interparticle interference peak.
§a, Interparticle distance according to Ehrenfest formula (see text for details).
¶N_{P0}, number of P0 molecules in a particle.
‖N_{SDS}, number of SDS molecules per particle.
**$N_{water\text{-}in}$, number of water molecules within the particle.
##Mass, mass of the particle.
§§Density, density of the particle.
‖‖Interparticle distances at $c = 1$ and 2 mg/ml were derived by assuming four P0 molecules. The parameters include $v'_{protein} = 0.74$ (Matthews, 1968), $v'_{SDS} = 0.886$ (Reynolds and Tanford, 1970a), $v'_{water} = 1$, $M_{w\text{-}P0} = 24{,}710$, $M_{w\text{-}SDS} = 288$, $M_{w\text{-}water} = 18$, $r_0 = 40$ Å. In the reciprocal range $>\sim 0.005$ Å^{-1}, the scattering intensity for $c = 6$ mg/ml P0 is similar to those at 1, 2, 4, and 8 mg/ml. This means that the particle structure factor from the former is similar to the others. Unlike the intensity data at 4 and 8 mg/ml, the interparticle peak does not show a clear peak, but rather a shoulder. The d-spacing refers to the edge position of the shoulder. Because of the measurement error for the peak position, the Bragg spacing may vary from $d = 245$ Å–276 Å. When the latter value was chosen, the aggregate number was 4.

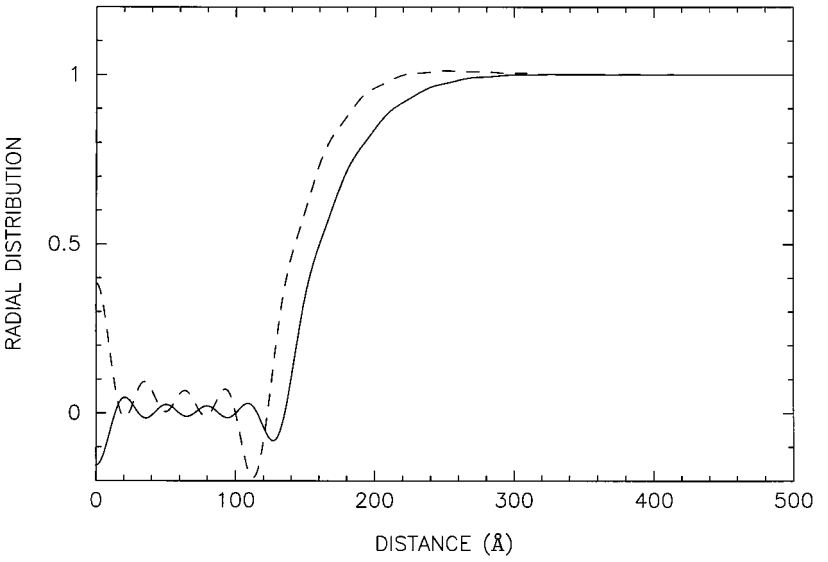

FIGURE 6 Calculated radial distribution function for 4 mg/ml P0 (*solid line*) and 8 mg/ml P0 (*dashed line*) from the interparticle structure factor (Fig. 5) as a function of the radial component of spherical coordinates (Å). Note that the flat region in the center is consistent with the spherical exclusion core of the particle.

set to $3.47 \times 10^{-3}/2$ and the Debye length to 73 Å. The temperature was 25°C and the dielectric constant of aqueous solution was 78.3. The total volume V (Å^3) that one particle may occupy was given by

$$V = M_{P0}10^4 N_{P0}/(6.0c_{P0}),$$

where M_{P0}, the molecular weight for P0, is 24,710; c_{P0}, the weight concentration in mg/ml, was either 4 or 8; and N_{P0}, the number of P0 molecules in a particle, was 4. The volume fractions for 4 and 8 mg/ml were 6.5×10^{-3} and 1.3×10^{-2}, respectively.

The intensity was calculated by varying the surface charge (or potential). The deviation between the observed and calculated scattering intensities was measured in terms of the R-factor. The effective particle size of σ' was then searched where the radial function (Fig. 6) gives the minimum value (see "Rescaled mean spherical approximation" in Appendix). The minimum R-factor was 6.9% for 4 mg/ml and 9.7% for 8 mg/ml P0, with 10 surface charges (surface potential 30 mV) for both solutions (Figs. 5 and 7). The calculated interparticle structure factors (Fig. 5) gave a maximum at the reciprocal coordinate which is close to, but not exactly at, the position of the observed interference peak (Figs. 2 and 7). Beyond this coordinate, where the interference becomes nearly 1, the intensity refers to the particle structure factor. Assigning the effective particle diameters to be 126 Å and 109 Å for the 4 and 8 mg/ml P0 samples, we calculated that the radial distribution $g(r)$ was nearly zero within the distance of the Debye length and particle size (73 Å + 80 Å) and became 1 beyond this distance (Fig. 6), indicating that the disposition of particles is like that in a dense gas. At low ionic strength (1.7×10^{-3}) the electrostatic repulsion is much stronger than the van der Waals attraction (Fig. 8). Thus, this repulsion force stabilizes the

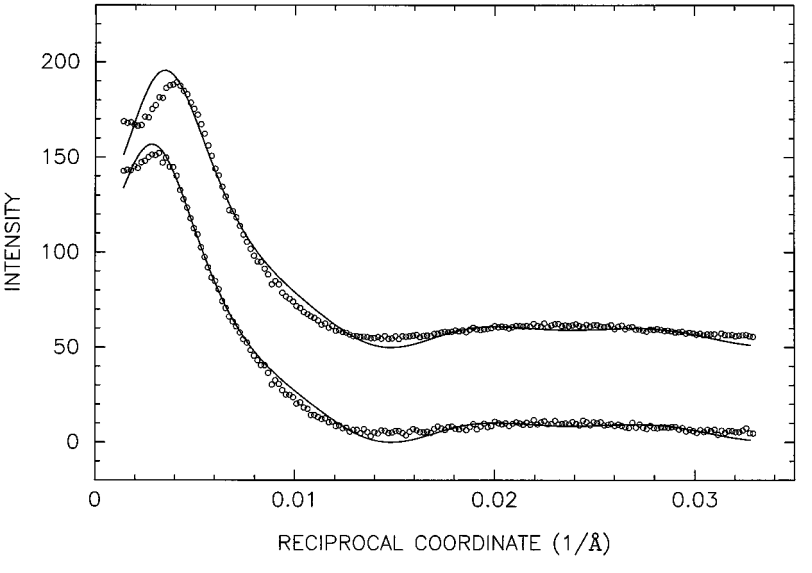

FIGURE 7 Comparison between the intensities for the observed and calculated solution scattering as a function of reciprocal coordinate (2 sin θ/λ, where 2θ is scattering angle and λ is x-ray wavelength). *Lower curves:* Data from P0 at 4 mg/ml in 0.1% SDS (*circles*) and intensity calculated from the particle structure factor (Fig. 5, *lower solid line*) and the Hayter-Penfold interference term (Fig. 5, *upper solid line*). The deviation between the curves is $R = 6.9\%$. *Upper curves:* Data from P0 at 8 mg/ml in 0.1% SDS circles) and intensity calculated from the particle structure factor (Fig. 5, *lower solid line*) and the Hayter-Penfold interference term (Fig. 5, *upper dashed line*). The deviation between the curves is $R = 9.7\%$.

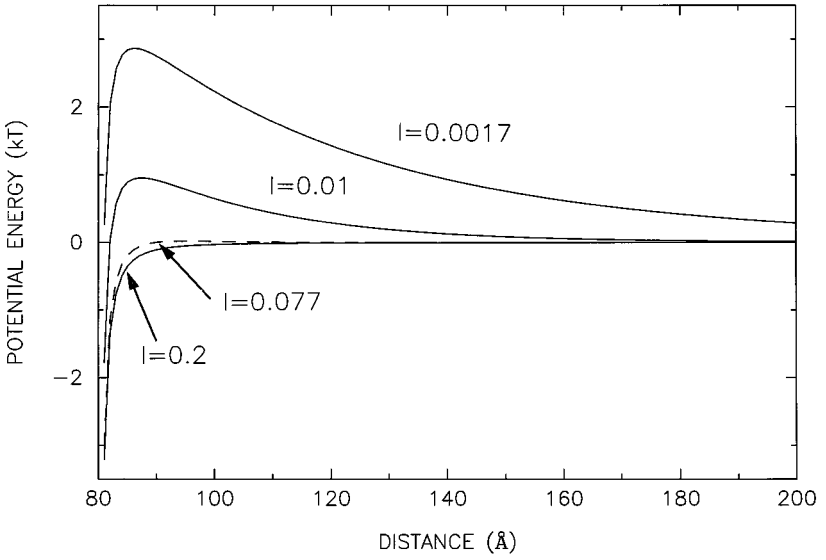

FIGURE 8 Total pair potential function as a function of distance between centers of a pair of spheres (Å) for different ionic strengths ranging from 1.7×10^{-3} to 0.2. The curve at the critical ionic strength 0.077 is indicated by the dashed line. The input parameters include particle size (80 Å), number of charges (10), volume fraction (6.5×10^{-3}), dielectric constant ($\epsilon = 78.3$), and temperature 25°C. The repulsive potential due to the mutual double-layer interaction at ionic strength 1.7×10^{-3} is nearly the same as the total potential curve, except near 80 Å, while the van der Waals attractive potential (with Hamaker coefficient 5.0×10^{-14} erg) is nearly the same as the total potential curve at the higher ionic strength of 0.2.

P0-SDS particles in solution. The consequence of this effect is that a rapid flocculation should occur when the ionic strength exceeds the critical limit (see Discussion).

Model of tetrameric assembly of P0 molecule

Bovine P0 glycoprotein has 219 amino acids, molecular weight 24,710 (excluding the N-linked oligosaccharide at Asn-93), and consists of three domains, i.e., extracellular, transmembrane, and cytoplasmic (Inouye and Kirschner, 1991). Assuming the extracellular and cytoplasmic domains to be spherical, and knowing the molecular weight and specific volume for dehydrated protein, we calculated the radii of these domains to be 16 Å and 13 Å, respectively (Table 2). For the extracellular domain this size is similar to that calculated from the atomic coordinates of the crystal structure (Shapiro et al., 1996) (Figs. 9 and 10). The 13 Å-radius of the cytoplasmic domain is consistent with the cytoplasmic separation of 30 Å between apposed myelin membranes (Inouye and Kirschner, 1988a; see Fig. 4). In the crystal, the P0 extracellular domains are assembled as a tetramer with an ~40 Å-separation between the monomers. Therefore, a tetramer of full sequence-P0 molecules is likely to be approximated by eight ~30 Å-diameter spheres separated by ~40 Å. These values are nearly the same as the 30 Å-particle size and the 43 Å-separation shown by the correlation function (Fig. 3).

TABLE 2 Physical and chemical characteristics of bovine P0

Domain	M_w*	Electrons	$N^{\#}$	$pI^{\S}$	r (Å)¶
P0	24,710	13,216	219	9.7	—
ext	14,091	7,513	1–124 (124)	5.3	16
lpg	2,627	1,420	125–150 (26)	—	—
cyt	7,992	4,283	151–219 (69)	11.5	13

The physicochemical characterization of the extracellular domain ($P0_{ext}$), transmembrane domain ($P0_{lpg}$), and cytoplasmic domain ($P0_{cyt}$) as derived from the amino acid sequence.

*M_w, molecular weight.

#N, residue position with number of residues in parentheses.

§pI, isoelectric pH.

¶r, radius of domain. The radius was derived according to $(4/3)\pi r^3 = M_w v'/A_v$, where M_w is shown above, $v' = 0.74$ cm^3/g (Matthews, 1968), and A_v is Avogadro's number. Note that the radius of the extracellular domain is similar to the one measured from the projection of the number of atoms (Fig. 10). Assuming α-helical conformation of the transmembrane domain, the length is 39 Å (1.5 Å × 26 residues), and the diameter is 10 Å. The separation between the extracellular and cytoplasmic domains therefore becomes 39 Å + 16 Å + 13 Å = 68 Å.

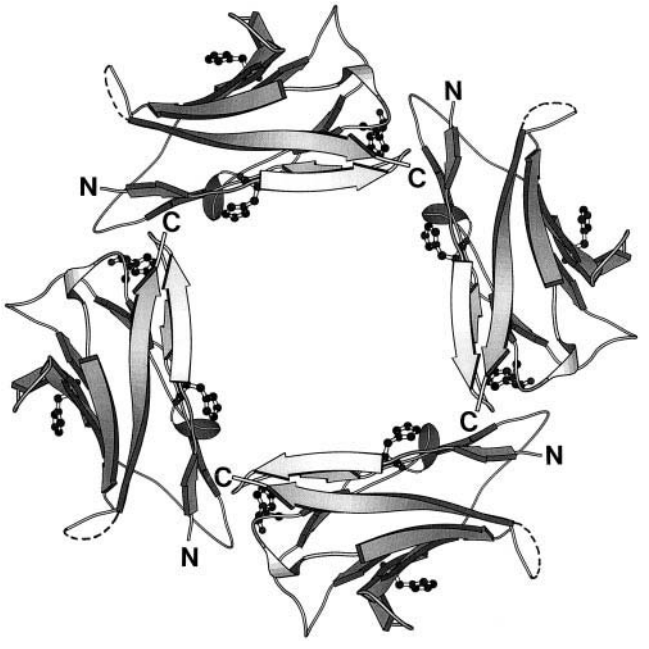

FIGURE 9 MOLSCRIPT (Kraulis, 1991) representation of the face-on view of the P0 tetramer (i.e., normal to the membrane surface) as derived from the atomic coordinates of the extracellular domain of P0 (Shapiro et al., 1996). Histidine residues are indicated by the balls and sticks. The loops indicated by the dashed lines are not defined by the crystallographic analysis.

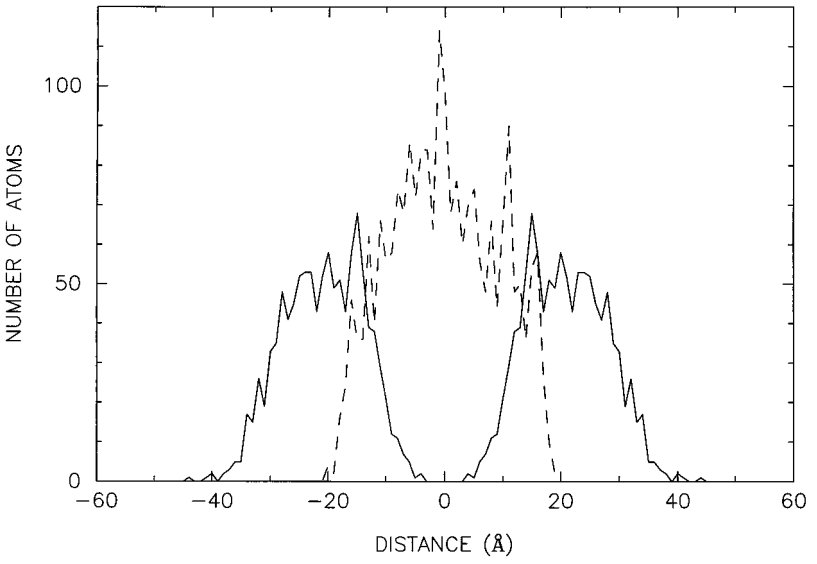

FIGURE 10 Projection along the fourfold rotation axis (*dashes*) and the axis normal to it of the number of atoms in the extracellular domain of P0 calculated from the atomic coordinates of a pair of apposed P0 molecules (Shapiro et al., 1996). The projection intervals are 1 Å steps. The distance between the monomers is ~40 Å, and the size of the monomer in either directions is ~30 Å. These values are similar to the ones determined from the correlation function of the solution scattering from P0 in 0.1% SDS (Fig. 3).

The model considered here assumes that the extracellular and cytoplasmic domains are solid spheres with radii r_{ext} = 16 Å and r_{cyt} = 13 Å, respectively, which are separated by a = 43 Å in the direction parallel to the surface of the membrane and by c = 68 Å in the transmembrane direction. The c value includes the length of the α-helical transmembrane P0 sequence, which consists of 26 residues (Table 2). When these eight spheres are assembled, the spherically averaged intensity as a function of the radial reciprocal coordinate is given by

$$\begin{aligned} I(R) = {} & 4(f_{ext}^2 + f_{cyt}^2) + 8\ \mathrm{sinc}(2\pi aR)(f_{ext}^2 + f_{cyt}^2) \\ & + 8 f_{ext} f_{cyt} \mathrm{sinc}(2\pi cR) \\ & + 4\ \mathrm{sinc}(2\pi(2)^{1/2} aR)(f_{ext}^2 + f_{cyt}^2) \\ & + 16 f_{ext} f_{cyt} \mathrm{sinc}(2\pi(c^2 + a^2)^{1/2} R) \\ & + 8 f_{ext} f_{cyt} \mathrm{sinc}(2\pi(c^2 + 2a^2)^{1/2} R), \end{aligned}$$

where f_{ext} and f_{cyt} are the structure factors for the hard spheres representing the extracellular and cytoplasmic domains, and R is the radial component of the spherical coordinate in reciprocal space. The initial R-factor comparing the observed and calculated x-ray intensity was 14.3%. In the nonlinear least-square analysis, the best result (with an R-factor of 10.4%) was obtained when r_{ext} and r_{cyt} were kept constant, a and c were varied initially, and subsequently all parameters were varied. The final optimized values were a = 39 Å, c = 59 Å, r_{ext} = 16 Å, and r_{cyt} = 13 Å.

To examine the sensitivity of the model parameters against the calculated intensity, two controls were examined. In one, three rather than four P0 molecules constituted the assembly, which otherwise maintained the same particle size and distances. In the other, the thickness c was reduced to 30 Å from 59 Å. For the particle constituted of three P0 molecules, the spherically averaged intensity is given by

$$\begin{aligned} I(R) = {} & 3(f_{ext}^2 + f_{cyt}^2) + 4\ \mathrm{sinc}(2\pi aR)(f_{ext}^2 + f_{cyt}^2) \\ & + 4 f_{ext} f_{cyt} \mathrm{sinc}(2\pi cR) \\ & + 2\ \mathrm{sinc}(2\pi(2)^{1/2} aR)(f_{ext}^2 + f_{cyt}^2) \\ & + 8 f_{ext} f_{cyt}\ \mathrm{sinc}(2\pi(c^2 + a^2)^{1/2} R) \\ & + 4 f_{ext} f_{cyt}\ \mathrm{sinc}(2\pi(c^2 + 2a^2)^{1/2} R). \end{aligned}$$

These models gave poorer fits (R = 15.6% and R = 19.4%, respectively) than the optimized structure (R = 10.4%).

The calculated intensity with the optimized parameters fit the observed intensity better in the low-angle region than in the wide-angle region (Fig. 11). The width of the space between the larger and smaller spheres, corresponding to the extracellular and cytoplasmic domains, was 30 Å [59 − (16 + 13)]. This value is about the same as the length of the hydrocarbon chains of two SDS molecules, which are oriented parallel to the c-direction. Given that an SDS chain has a length of 16 Å and a surface area of 22 Å^2, the volume of an SDS molecule is 350 Å^3 (Israelachvili, 1992). The space between the spheres, i.e., corresponding to the region of the transmembrane domain, has a volume of 45,630 Å^3 = [(59 − 16 − 13) Å × 39 Å × 39 Å]. If SDS molecules fill this space, then the number of SDS molecules in the 80 Å-diameter particle is 130. This value is similar to the estimated 171 SDS molecules at 2 mg/ml P0 concentration.

DISCUSSION

Tetrameric assembly of P0 glycoprotein

What is the molecular basis for the extensive intermembrane adhesion in nerve myelin? This adhesion is particularly evident in internodal compact myelin where the mem-

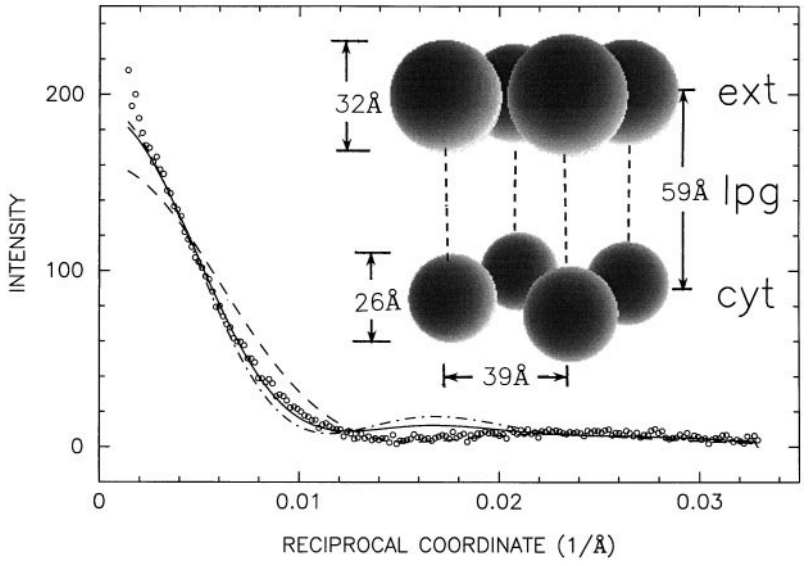

FIGURE 11 Comparison between the observed solution scattering (*circles*) from P0 (at 2 mg/ml in 0.1% SDS) and the intensity (*solid line*) calculated from the model of the P0 tetramer. The curves are plotted as a function of reciprocal coordinate (2 sin θ/λ, where 2θ is the scattering angle and λ is x-ray wavelength), and are normalized to unity. The latter intensity was calculated using the optimized parameters $a = 39$ Å (the distance between the spheres on the membrane surface), $c = 59$ Å (the distance between the spheres across the transmembrane space), $r_{ext} = 16$ Å (radius of extracellular domain), and $r_{cyt} = 13$ Å (radius of cytoplasmic domain). The inset indicates a schematic model of the full-sequence P0 molecule arranged tetramerically, with the larger spheres above and the smaller spheres below corresponding to the extracellular and cytoplasmic domains, respectively. The dotted line interconnecting each pair of spheres represents the transmembrane domain, which has not been included in the modeling. The calculated intensities for the two control models are indicated: (*dashes* and *dots*) three P0 molecules constitute the assembly having the same dimensions as the P0 tetramer; and (*dashes*) tetrameric assembly has a c thickness reduced to 30 Å from 59 Å. Note that the first control model fits the observed intensity at reciprocal coordinates <0.014 Å^{-1}, while the second control model fits better at wider angle. The tetrameric model depicted in the inset gives a calculated intensity which most closely fits the observed intensity.

branes are closely apposed at both their cytoplasmic and extracellular surfaces. In a previous study we approached this question by tabulating the data for myelin lipid and protein composition and relating it to the intermembrane separations as directly measured by x-ray diffraction (Inouye and Kirschner, 1988a, b). Aided by DLVO theory for colloid stability (Ninham and Parsegian, 1971), we were able to account for the swelling behavior of myelin based on its chemical constituents; however, we were unable to explain the native period under physiological conditions, since the model calculation gave larger periods than were obtained experimentally. Moreover, at neutral pH a structural transition from a swollen to a native period structure was observed, suggesting that the deprotonation of histidine residues may play a significant role in the stability of the native structure. Analyses of myelin protein sequences (Inouye and Kirschner, 1991) revealed similar β propensity curves between the extracellular domain of P0 and the V_H domain of M603 immunoglobulin (Inouye and Kirschner, 1991). This led us to propose a model for the extracellular domain of P0 (Wells et al., 1993) and for the P0-P0 homotypic interactions that could underlie intermembrane adhesion in myelin. The subsequent x-ray crystallographic structure of this domain of P0 to atomic resolution (Shapiro et al., 1996) showed, as we had predicted, that the asymmetric unit was similar to the known structure of the immunoglobulin variable region.

A novel aspect of the x-ray crystallographic findings is that the crystals of the extracellular domain of P0 molecule belong to the space group I422, which has high symmetry and is very rare. The molecular interfaces in the crystal reveal P0-P0 contacts within a narrow, ~46-Å-wide space, which is similar to the extracellular separation in normal nerve myelin. In the crystal, deprotonated histidine residues are located in the region of P0-P0 contact, which may explain the discontinuous compaction at neutral pH in PNS myelin (Inouye and Kirschner, 1988a). Based on evidence from analytical ultracentrifugation, which was used to examine the assembly of P0 monomers in solution, Shapiro et al. (1996) proposed that there is a network of tetramerically arrayed P0 molecules in intact nerve myelin. The P0:lipid molar ratio of such a network is calculated to be 1:52 (Shapiro et al., 1996), which is similar to the 1:86 derived from chemical composition (Inouye and Kirschner, 1988b). Whether the proposed tetrameric assembly actually exists in nerve myelin was not addressed in the crystallographic study. Our synchrotron x-ray scattering study indicates that such a tetramer of full-sequence P0 does exist in the membrane bilayer-mimetic environment of 0.1% SDS.

Surface charge

Using liquid theory (Hayter and Penfold, 1981a, b), we showed here that the observed interparticle interference is

explained by the known parameters of volume available for a particle (which is inverse to the number density), temperature, and dielectric constant of the medium. Since the number of P0 and SDS molecules are known from the chemical composition (Table 1), it is useful to compare the calculated and measured numbers of charges. The number per P0 molecule ($pI = 9.7$) at pH 7.4 was estimated to be +10. Because SDS molecules bound to P0 carry one negative charge per SDS molecule, the number of charges of the tetrameric assembly of P0 with SDS are −47 for 4 mg/ml and +2 for 8 mg/ml P0. These values from the model appear to be different from the measured value of −10 from the scattering data.

One reason for this discrepancy may be the partial ionization (~3–25%) for charged moieties of SDS (Hayter and Penfold, 1981b). A similar reduction of charges or renormalization has been observed for other systems, e.g., cytochrome C (Wu and Chen, 1988), highly charged polystyrene latex (Alexander et al., 1984), and nerve myelin membrane (Inouye and Kirschner, 1988b). For myelin, the reduced surface charge density may be explained both by the binding effect of ions (rather than counterion screening of ionizable residues) and by the space charge approximation for a low dielectric fuzzy coat on the surface (Inouye and Kirschner, 1988b). An additional reason for this discrepancy may be that the positive charged cytoplasmic domain of P0 might be effectively sealed from the aqueous medium, or neutralized by tightly bound negatively charged molecules, e.g., residual phospholipid or ions.

Electrostatic effect on P0 protein in SDS solution

In the current ionic environment with low ionic strength 1.7×10^{-3} (the Debye length is 73 Å) the electrostatic repulsion between two spheres (Fig. 8) is much stronger than the van der Waals attraction. When the ionic strength becomes higher, the electrostatic repulsion decreases, and a rapid flocculation (i.e., condensation) may occur due to strong attraction. For a pair of spheres having diameter σ with a distance between their centers r, the electrostatic repulsive V_r (see Eq. 14 in Appendix) and attractive potential V_a (Verwey and Overbeek, 1948) can be written as

$$V_r = \pi\epsilon_0\epsilon\sigma^2\varphi_0^2\exp[-\kappa(r-\sigma)]/r$$

$$V_a = A\{2/(s^2-4) + 2/s^2 + \ln[(s^2-4)/s^2]\}/6$$

where A is the Hamaker coefficient (5.0×10^{-14} erg; Ninham and Parsegian, 1971), and $s = r/(\sigma/2)$. Putting $D = r - \sigma$ in which D is the shortest distance between the two spheres, and assuming $D \ll \sigma/2$, V_a may be approximated by $V_a = A\sigma/[24(r-\sigma)]$ (Verwey and Overbeek, 1948). The total potential is given by

$$V_t = V_r - V_a.$$

The critical ionic condition for flocculation should satisfy the following conditions:

$$V_t = 0 \quad \text{and} \quad dV_t/dr = 0.$$

From the first condition,

$$\pi\epsilon_0\epsilon\sigma^2\varphi_0^2\exp[-\kappa(r-\sigma)]/r = A\sigma/[24(r-\sigma)].$$

From the second condition,

$$\kappa + 1/r = 1/(r-\sigma) \quad \text{or} \quad r = [\sigma + (\sigma^2 + 4\sigma/\kappa)^{1/2}]/2.$$

From these two equations and given a constant surface charge of 10 for an 80 Å-diameter spherical particle, dielectric constant (78.3), and temperature (25°C), we numerically determined that the critical value of ionic strength was 0.077 and the distance between a pair of particles where $V_t = 0$ was 90 Å. At this ionic strength the P0-SDS particles should precipitate as an aggregate.

As observed for globular and soluble immunoglobulin (Termine et al., 1972), a one-dimensional array of tetrameric P0 assemblies at the critical ionic strength may morphologically resemble amyloid fibers since their cross-sectional view (Fig. 9) is similar to that for certain Aβ fibers in which the β chains run nearly tangential to the tube, and the intersheet interaction is in the radial direction (Inouye et al., 1993). Such an array of P0 molecules, organized as a tube running normal to the membrane faces, may mediate membrane stacking in the nerve myelin sheath.

Protein-SDS complex

Previous studies on protein-SDS complexes indicate different models for their structure. In the prolate ellipsoidal model (Reynolds and Tanford, 1970a, b; Cantor and Schimmel, 1980), the complex is a solid ellipsoid in which the semi-minor axis is a constant 18 Å for any protein, while the major axis is proportional to the length of the polypeptide chains. This model is not supported by either neutron scattering (Bendedouch et al., 1983; Chen and Teixeira, 1986; Guo et al., 1990; Ibel et al., 1990; Sjöberg et al., 1987) or x-ray scattering (Daban et al., 1991; Hirai et al., 1993; Itri and Amaral, 1990, 1991; Samsó et al., 1995), which support, rather, an alternative "necklace" model (Shirahama et al., 1974). In this model (Samsó et al., 1995), which is based on cryoelectron microscopy and small-angle x-ray scattering, the polypeptide chains are unfolded, and dispersed along them are ~57–62-Å-diameter particles that are slightly larger than pure SDS micelles. Whether this model for complexes of extrinsic proteins with SDS also applies to complexes of membrane proteins with SDS is questionable. Our current results show that the P0-SDS complex is a nearly spherical structure having a diameter of 80 Å for different concentrations of the protein in 0.1% SDS solution. The exclusion length of proteins should increase upon denaturation by SDS. That this did not occur here indicates that the SDS molecules in salt-free water likely mimic the lipid bilayer and do not denature the protein, unlike their effect on extrinsic proteins (Hjertén et al., 1988, Papavoine et al., 1994). The SDS molecules apparently solvate the hydrophobic, transmembrane domains of the protein, and

preserve the native folding in the aqueous (extracellular and cytoplasmic) domains.

Myelin cytoplasmic apposition

The crystallographic study of the extracellular domain of P0 glycoprotein shows that this domain forms tetrameric assemblies in the crystal (Shapiro et al., 1996). The synchrotron x-ray scattering analysis presented here indicates that the *whole* P0 molecule in solution, after solubilization with a lipid mimetic, also assembles tetramerically. The folding of the cytoplasmic domain, whose structure has not yet been solved crystallographically, is constrained both by the tetrameric assembly of the extracellular domain, to which it is linked, and also by the narrow intermembrane gap of 30 Å at the cytoplasmic apposition of myelin membranes. The cytoplasmic apposition was proposed to be mediated by ionic interactions between P0 and lipid polar headgroups (Lemke, 1988); however, such an explanation is not consistent with experimental data that the cytoplasmic separation in myelin remains virtually unaltered across wide variations of pH and ionic strength (Inouye and Kirschner, 1988a). Rather, we suggest that this very stable apposition may depend on lipid-anchoring of the protein and additional hydrophobic interactions between P0 cytoplasmic domains of apposed membranes. Such a model is consistent with the current measurement of effective surface charge (see above), suggesting that the positive charged cytoplasmic domain is effectively sealed from the aqueous medium by tightly bound phospholipids or ions. In particular, P0 is palmitoylated at the cytoplasmic Cys-153 (Bizzozero et al., 1994). This residue may be oriented in myelin near the membrane surface to enable hydrophobic interactions between oppositely directed, ~20-Å-long palmitate hydrocarbon chains. Amphiphilic α-helical sequences and hydrophobic side chains of β-strands, which are predicted secondary structure elements in the cytoplasmic domain of P0 (Inouye and Kirschner, 1991), may further stabilize a hydrophobic pocket in the middle of the cytoplasmic apposition.

Future studies

One of the aims of our current research efforts is to crystallize full-length P0 (Sedzik et al., 1998b; J. Sedzik, Y. Kotake, and K. Uyemura, submitted for publication). While the soluble domains of membrane proteins and several integral membrane proteins are routinely used for crystallization, to our knowledge no integral membrane proteins containing a *single* transmembrane domain has ever been successfully crystallized. This may be due to the flexibility of the single transmembrane helix connecting the cytoplasmic and extracellular domains. In terms of crystal growth it is significant that, as demonstrated here, a low concentration of SDS, which mimics a biological membrane, may be used for solubilization without denaturing the protein.

Mutations in P0 protein can cause serious neurological disorders (Uyemura et al., 1994; Warner et al., 1996), arising from conformational changes in the mature protein that has already been incorporated in the membrane, or from disruption of the normal biosynthesis of the nerve myelin by the mutated proteins. In either case, the myelin membrane structure and membrane-membrane interactions will be altered. The solution scattering system and methodology that we have developed here can be applied to these pathological P0s to examine possible alterations of molecular assembly and structure and interactions in solution with other myelin proteins, i.e., myelin basic protein.

APPENDIX

X-ray diffraction theory of protein in solution

Given a spherically symmetric particle the phase changes at the intensity minima. With $A_s(R) = \pm[I(R)]^{1/2}$ where $I(R)$ is the scattering intensity of the particle as a function of radial component in the reciprocal spherical coordinate R, the electron density projection in the radial direction $\rho(r)$ as a function of radial component in the real space r is given by

$$\rho(r) = 4\pi \int R^2 A_s(R)\sin(2\pi rR)/(2\pi rR)dR. \qquad (1)$$

The intensity $I(R)$ can be written as

$$I(R) = \left[4\pi \int \rho(r) r^2 \sin(2\pi rR)/(2\pi rR)dr\right]^2 \qquad (2)$$

Using the atomic factors or form factors for a sphere, the intensity function (Debye equation) can be written as

$$I(R) = \sum\sum f_m(R) f_n(R)\sin(2\pi r_{mn}R)/(2\pi r_{mn}R), \qquad (3)$$

where $f_m(R)$ is a structure factor of the mth unit object, and $r_{mn} = |\mathbf{r}_m - \mathbf{r}_n|$. When the unit object is a hard sphere having a radius r_0, the structure factor is given by

$$f(R) = \langle\rho\rangle 3v j_1(2\pi r_0 R)/(2\pi r_0 R), \qquad (4)$$

where $\langle\rho\rangle$ is the uniform density of the hard sphere, v is its volume, and $j_1(x) = (\sin x - x\cos x)/x^2$.

In Eq. 3 the double sum refers to the interference term. When the two point atoms are separated by a, the intensity can be expressed as

$$I(R) = 2[1 + \sin(2\pi aR)/2\pi aR]. \qquad (5)$$

The correlation function $z(r)$ and the Guinier plot (Guinier and Fournet, 1955; Guinier, 1963) are calculated directly from the observed intensity. The correlation function $z(r)$, which is the self-convolution of the scattering particle in spherical coordinates, is defined by

$$z(r) = 4\pi \int R^2 I(R)\sin(2\pi rR)/(2\pi rR)dR. \qquad (6)$$

The term $r^2 z(r)$ is often used and termed a distance distribution function.

Charged sphere liquid model

The charged sphere liquid theory in the mean spherical approximation (closed form given by Hayter and Penfold, 1981a; Hayter and Hansen,

1982) explicitly relates the electrostatic repulsion potential in a Yukawa form according to DLVO theory (Verwey and Overbeek, 1948; Inouye and Kirschner, 1988a) to the radial distribution function via the Ornstein-Zernike equation, and allows one to measure the surface charge from the observed synchrotron x-ray solution scattering. We apply this liquid model to the interparticle interference here.

For spherically symmetric particles the scattering intensity $I(R)$ is written as

$$I(R) = NF^2(R)S(R), \tag{7}$$

where N is the number of particles, $F(R)$ is the particle structure factor, and $S(R)$ is interparticle interference. By using the radial distribution function $g(r)$, $S(R)$ may be written as

$$S(R) = 1 + (1/\nu)\int 4\pi r^2(g(r) - 1)\sin(2\pi rR)/(2\pi rR) \tag{8}$$

and

$$g(r) = 1 + \nu\int 4\pi R^2(S(R) - 1)\sin(2\pi rR)/(2\pi rR). \tag{9}$$

We define $K = 2\pi R\sigma = Q\sigma$, where σ is the diameter of the sphere, $r/\sigma = x$, and $\nu = 1/n = \pi\sigma^3/(6\eta)$, where n is number density and η is volume fraction. Substituting R, r, and ν by K, x, and η gives the formula in dimensionless units,

$$S(K) = 1 + 24\eta\int x^2(g(x) - 1)\sin Kx/Kx\, dx \tag{10}$$

and

$$g(x) = 1 + (1/12\pi\eta)\int K^2(S(K) - 1)\sin Kx/Kx\, dK. \tag{11}$$

The total correlation function is defined as $h(x) = g(x) - 1$, which is related to the direct correlation function $c(x)$ by the Ornstein-Zernike equation

$$h(x) = c(x) + n\sigma^3\int h(|\mathbf{x} - \mathbf{y}|)c(y)d\mathbf{y}. \tag{12}$$

The direct correlation function is defined by the pair potential function $u(x)$ in the mean spherical approximation (MSA) according to

$$c(x) = -\beta u(x), \quad x > 1, \quad \text{and} \quad h(x) = -1, \quad x < 1, \tag{13}$$

where $\beta = 1/k_BT$, k_B is the Boltzman constant, and T is absolute temperature. Here the pair potential $u(x)$ is written in the Yukawa form by

$$\beta u(x) = \gamma\exp(-kx)/x, \quad x > 1,$$

and

$$\beta u(x) = \infty, \quad x < 1. \tag{14}$$

The term $\gamma\exp(-k) = \beta\pi\epsilon_0\epsilon\sigma\varphi_0^2$ is a coupling constant, and $k = \kappa\sigma$ using the inverse of Debye length with dielectric constant $4\pi\epsilon_0\epsilon \rightarrow \epsilon$ given by

$$\kappa = (8\pi e^2IN_A/10^3\epsilon k_BT)^{1/2}. \tag{15}$$

Here, e is elementary charge, I is ionic strength, N_A is Avogadro's number, and φ_0 is surface potential. The coupling constants can be derived from the surface potential $\varphi_0 = (ze/[\pi\epsilon_0\epsilon\sigma(2 + \kappa\sigma))$ or from the number of charges z according to

$$\gamma\exp(-k) = 2.0148 \times 10^{-4}\epsilon\sigma\varphi_0^2/T = 1.6711 \times 10^5z^2/[\epsilon\sigma T(1 + k/2)^2], \tag{16}$$

where the surface potential φ_0 is in mV, z is the number of charges, σ is in Å, ϵ is the dielectric constant, and T is the absolute temperature (Hayter and Hansen, 1982). Hayter and Penfold (1981a) derived $c(x)$ and $S(K)$ in closed form.

Rescaled mean spherical approximation (RMSA)

Using the MSA approximation for charged spheres having a low volume fraction may yield an unphysical, negative radial distribution function (Hansen and Hayter, 1982). The rescaled MSA model defines the parameter σ' (effective hard core size) where $g(\sigma')$ is close to zero (Hansen and Hayter, 1982). The interparticle structure factor $S(R)$ was calculated for reduced dimensionless parameters. The structure factor $S(\eta, \gamma, k, K)$ of the physical system may thus be accurately calculated by evaluating $S(\eta', \gamma', k', K')$ for the rescaled system, and then trivially resealing the result by a contraction of the reduced wave numbers $K' = Q\sigma'$ to the relevant scale $K = Q\sigma = K'\sigma/\sigma'$, where $Q = 2\pi R$ is the momentum transfer.

Physical parameters of SDS-protein complex

Consider a spherical particle with a radius r_o and which is composed of protein, SDS, and water. The interparticle space is assumed to be entirely composed of water. When the particles are monodispersed in solution, and the center-to-center distance between them is a, the volume occupied by one particle is V, while the individual particle volume is $v = 4\pi r_0^3/3$. The total volume V is given by $0.71a^3$ from the volume fraction in a face-centered cubic lattice (Guinier and Fournet, 1955). The particle volume is determined by the sum of the individual volumes of its components (protein, SDS, and water):

$$V = V_{\text{water-out}} + v,$$

where

$$v = V_{\text{water-in}} + V_{\text{SDS}} + V_{\text{P0}} \tag{17}$$

Here, $V_{\text{water-out}}$ is the volume of water outside the particle, and $V_{\text{water-in}}$ is that inside the particle. The corresponding weight formula is

$$W = W_{\text{water-out}} + (W_{\text{water-in}} + W_{\text{SDS}} + W_{\text{P0}}) = V_{\text{water-out}}/v'_{\text{w}} + (V_{\text{water-in}}/v'_{\text{w}} + V_{\text{SDS}}/v'_{\text{SDS}} + V_{\text{P0}}/v'_{\text{P0}}) \tag{18}$$

where v'_{w}, v'_{SDS}, and v'_{P0} are specific volumes for water, SDS, and P0. The concentrations of the protein and SDS in units of weight/volume, W_{P0} and W_{SDS}, are given by

$$w'_{\text{P0}} = W_{\text{P0}}/V \quad \text{and} \quad w'_{\text{SDS}} = W_{\text{SDS}}/V \tag{19}$$

Thus, the number of protein and SDS molecules within a particle is

$$N_{\text{P0}} = A_vW_{\text{P0}}/M_{\text{P0}} = A_vVw'_{\text{P0}}/M_{\text{P0}},$$

and

$$N_{\text{SDS}} = A_vVw'_{\text{SDS}}/M_{\text{SDS}}. \tag{20}$$

where A_v is Avogadro's number, and M_{P0} and M_{SDS} are molecular weights for P0 and SDS, respectively.

Then,

$$V_{\text{water-in}} = v - V(w'_{\text{SDS}}v'_{\text{SDS}} + w'_{\text{P0}}v'_{\text{P0}}),$$

and (21)

$$N_{\text{water-in}} = A_{\text{v}}V_{\text{water-in}}/(M_{\text{water}}v'_{\text{w}})$$

The specific volume of the particle v' is given by

$$1/v' = 1 + V/v\{(1 - v'_{\text{P0}})w'_{\text{P0}} + (1 - v'_{\text{SDS}})w'_{\text{SDS}}\}; \quad (22)$$

and the mass per V is given by

$$M_{\text{mass}} = N_{\text{P0}}M_{\text{P0}} + N_{\text{SDS}}M_{\text{SDS}} + N_{\text{water-in}}M_{\text{water}}. \quad (23)$$

We thank Dr. Y. Kotake for the phosphorus measurements and Dr. Jeff Penfold for the Fortran source code for the Hayter-Penfold structure factor. We also thank an anonymous referee for valuable suggestions regarding the two control models.

This research was supported by grants from the Royal Swedish Academy of Science (to J.S.), the Japanese Society of Promotion of Science (to J.S.), MFR (to J.S.), and Ministry of Education (to K.U.). Travel support was provided by the Chancellor of Uppsala University (to J.S.). The solution x-ray scattering measurements were performed during the staff priority time assigned to Dr. H. Tsuruta at SSRL, which is operated by the US Department of Energy (DOE), Office of Basic Energy Sciences. The SSRL Biotechnology Program is supported by the National Institutes of Health, National Center for Research Resources, Biomedical Technology Program, and by the DOE Office of Biological and Environmental Research. Research at Boston College was supported by Institutional Research Support Funds and by a grant from the Guillain-Barré Syndrome Foundation International (to D.A.K.).

REFERENCES

Alexander, S., P. M. Chaikin, P. Grant, G. J. Morales, and P. Pincus. 1984. Charge renormalization, osmotic pressure, and bulk modulus of colloidal crystals: theory. *J. Chem. Phys.* 80:5776–5781.

Bartlett, G. R. 1959. Phosphorus assay in column chromatography. *J. Biol. Chem.* 234:466–468.

Bendedouch, D., S-H. Chen, and W. C. Koehler. 1983. Determination of interparticle structure factors in ionic micellar solutions by small angle neutron scattering. *J. Phys. Chem.* 87:2621–2628.

Bizzozero, O. A., K. Fridal, and A. Pastuszyn. 1994. Identification of the palmitoylation site in rat myelin P0 glycoprotein. *J. Neurochem.* 62: 1163–1171.

Blaurock, A. E. 1971. Structure of the nerve myelin membrane: proof of the low-resolution profile. *J. Mol. Biol.* 56:35–52.

Cantor, C. R., and P. R. Schimmel. 1980. Biophysical Chemistry. W. H. Freeman and Co., New York.

Chen, S.-H., and J. Teixeira. 1986. Structure and fractal dimension of protein-detergent complexes. *Phys. Rev. Lett.* 57:2583–2586.

Daban, J.-R., M. Samso, and S. Bartolome. 1991. Use of Nile red as a fluorescent probe for the study of the hydrophobic properties of protein-sodium dodecyl sulfate complexes in solution. *Anal. Biochem.* 199: 162–168.

Guinier, A. 1963. X-Ray Diffraction. W.H. Freeman and Co., New York.

Guinier, A., and G. Fournet. 1955. Small-Angle Scattering of X-Rays. John Wiley and Sons., Inc., New York.

Guo, X. H., N. M. Zhao, S. H. Chen, and J. Teixeira. 1990. Small-angle neutron scattering study of the structure of protein/detergent complexes. *Biopolymers.* 29:335–346.

Hansen, J.-P., and J. B. Hayter. 1982. A rescaled MSA structure factor for dilute charged colloidal dispersions. *Mol. Phys.* 46:651–656.

Hayter, J. B., and J.-P. Hansen. 1982. The structure factor of charged colloidal dispersions at any density. Institut Laue-Langevin Report No. 82HA14T.

Hayter, J. B., and J. Penfold. 1981a. An analytic structure factor for macro-ion solutions. *Mol. Phys.* 42:109–118.

Hayter, J. B., and J. Penfold. 1981b. Self-consistent structural and dynamic study of concentrated micelle solutions. *J. Chem. Soc. Faraday Trans. I.* 77:1851–1863.

Hirai, M., R. Kawai-Hirai, T. Hirai, and T. Ueki. 1993. Structural changes of jack bean urease induced by addition of surfactants studied with synchrotron-radiation small-angle x-ray scattering. *Eur. J. Biochem.* 215:55–61.

Hjertén, S., M. Sparrman, and J.-L. Liao. 1988. Purification of membrane proteins in SDS and subsequent renaturation. *Biochim. Biophys. Acta.* 939:476–484.

Hoeflmayr, J., and R. Fried. 1966. Eine Methode zur routinemäßigen Bestimmung des Lipidphosphors und der Phosphatide. Medizin und Ernährung. 7:9–10.

Ibel, K., R. P. May, K. Kirschner, H. Szadkowski, E. Mascher, and P. Lundahl. 1990. Protein-decorated micelle structure of sodium-dodecyl-sulfate-protein complexes as determined by neutron scattering. *Eur. J. Biochem.* 190:311–318.

Inouye, H., P. E. Fraser, and D. A. Kirschner. 1993. Structure of β-crystallite assemblies formed by Alzheimer β-amyloid protein analogues: analysis by x-ray diffraction. *Biophys. J.* 64:502–519.

Inouye, H., and D. A. Kirschner. 1988a. Membrane interactions in nerve myelin. I. Determination of surface charge from effects of pH and ionic strength on period. *Biophys. J.* 53:235–246.

Inouye, H., and D. A. Kirschner. 1988b. Membrane interactions in nerve myelin. II. Determination of surface charge from biochemical data. *Biophys. J.* 53:247–260.

Inouye, H., and D. A. Kirschner. 1991. Folding and function of the myelin proteins from primary sequence data. *J. Neurosci. Res.* 28:1–17.

Inouye, H., H. Tsuruta, D. A. Kirschner, J. Sedzik, and K. Uyemura. 1998. Tetrameric assembly of full sequence P0 myelin glycoprotein by synchrotron radiation. Abstracts of 4th International School and Symposium on Synchrotron Radiation in Natural Science, June 15–20, 1998. Ustron-Jaszowiec, Poland, p. 31.

Israelachvili, J. N. 1992. Intermolecular and Surface Forces. Academic Press, London.

Itri, R., and L. Q. Amaral. 1990. Study of the isotropic-hexagonal transition in the system SDS/H_2O. *J. Phys. Chem.* 94:2198–2202.

Itri, R., and L. Q. Amaral. 1991. Distance distribution function of sodium dodecyl sulfate micelles by x-ray scattering. *J. Phys. Chem.* 95: 423–427.

Kirschner, D. A., H. Inouye, A. L. Ganser, and V. Mann. 1989. Myelin membrane structure and composition correlated: a phylogenetic study. *J. Neurochem.* 53:1599–1609.

Kirschner, D. A., H. Inouye, and R. A. Saavedra. 1996. Membrane adhesion in peripheral myelin: good and bad wraps with protein P0. *Structure.* 4:1239–1244.

Kratky, O., and K. Müller. 1982. Aggregation and micellar structures of small molecules in solution. *In* Small Angle X-ray Scattering. O. Glatter and O. Kratky, editors. Academic Press, London. 499–510.

Kraulis, P. J. 1991. MOLSCRIPT: a program to produce both detailed and schematic plots of protein structures. *J. Appl. Crystallogr.* 24:946–950.

Lemke, G. 1988. Unwrapping the genes of myelin. *Neuron.* 1:535–543.

Matthews, B. W. 1968. Solvent content of protein crystals. *J. Mol. Biol.* 33:491–497.

Ninham, B. W., and V. A. Parsegian. 1971. Electrostatic potential between surfaces bearing ionizable groups in ionic equilibrium with physiologic saline solution. *J. Theoret. Biol.* 31:405–428.

Norton, W. T. 1974. Isolation of myelin from nerve tissue. *Methods Enzymol.* 31:435–444.

Papavoine, C. H. M., R. N. H. Konings, C. W., Hilbers, and F. J. M. van de Ven. 1994. Location of M13 coat protein in sodium dodecyl sulfate micelles as determined by NMR. *Biochemistry.* 22:12990–12997.

Reiss-Husson, F., and V. Luzzati. 1964. The structure of the micellar solutions of some amphiphilic compounds in pure water as determined by absolute small-angle x-ray scattering techniques. *J. Phys. Chem.* 68:3504–3511.

Reiss-Husson, F., and V. Luzzati. 1966. Small-angle x-ray scattering study of the structure of soap and detergent micelles. *J. Colloid Interface Sci.* 21:534–546.

Reynolds, J., and C. Tanford. 1970a. The gross conformation of protein-sodium dodecyl sulfate complexes. *J. Biol. Chem.* 245:5161–5165.

Reynolds, J., and C. Tanford. 1970b. Binding of dodecyl sulfate to proteins at high binding ratios: possible implications for the state of proteins in biological membranes. *Proc. Natl. Acad. Sci. USA.* 66:1002–1007.

Sakamoto, Y., K. Kitamura, K. Yoshimura, T. Nishijima, and K. Uyemura. 1987. Complete amino acid sequence of P0 protein in bovine peripheral nerve myelin. *J. Biol. Chem.* 262:4208–4214.

Samsó, M., J-R. Daban, S. Hansen, and G. R. Jones. 1995. Evidence for sodium dodecyl sulfate/protein complexes adopting a necklace structure. *Eur. J. Biochem.* 232:818–824.

Sedzik, J., Y. Kotake, and K. Uyemura. 1997. Purification of P0 protein for crystallization. *J. Neurochem.* 69 (Suppl.):84D.

Sedzik, J., Y. Kotake, and K. Uyemura. 1998a. Purification of the PASII/PMP22—extremely hydrophobic glycoprotein of myelin membrane. *NeuroReport.* 9:1595–1600.

Sedzik, J., K. Uyemura, and M. Ataka. 1998b. Phase diagram deduced from factorially designed 3-D crystallization trials pinpoints crystallization conditions of extremely hydrophobic myelin membrane glycoprotein. Abstracts of 7th International Conference on the Crystallization of Biological Macromolecules, Granada, Spain, May 3–8, p. 116.

Shapiro, L., J. P. Doyle, P. Hensley, D. R. Colman, and W. A. Hendrickson. 1996. Crystal structure of the extracellular domain from P0, the major structural protein of peripheral nerve myelin. *Neuron.* 17: 435–449.

Shirahama, K., K. Tsuji, and T. Takagi. 1974. Free-boundary electrophoresis of sodium dodecyl sulfate-protein polypeptide complexes with special reference to SDS-polyacrylamide gel electrophoresis. *J. Biochem. (Tokyo).* 75:309–319.

Sjöberg, B., S. Pap, and J. Göteborg. 1987. Dodecylsulfate-induced dissociation of human alpha2-macroglobulin: an investigation using small-angle neutron scattering and the equilibrium dialysis technique. *Eur. J. Biochem.* 162:259–264.

Termine, J. D., E. D. Eanes, D. Ein, and G. G. Glenner. 1972. Infrared spectroscopy of human amyloid fibrils and immunoglobulin proteins. *Biopolymers.* 11:1103–1113.

Uyemura, K., K. Kitamura, and M. Miura. 1992. Structure and molecular biology of P0 protein. *In* Myelin: Biology and Chemistry, R. Martenson, editor. CRC Press, Boca Raton. 481–508.

Uyemura, K., Y. Takeda, and H. Asou. 1994. Neural cell adhesion proteins and neurological diseases. *J. Biochem. (Tokyo).* 116:1187–1192.

Verwey, E. J. W., and J. Th. G. Overbeek. 1948. Theory of the stability of lyophobic colloids. Elsevier, New York.

Wakatsuki, S., K. O. Hodgson, D. Eliezer, M. Rice, S. Hubbard, N. Gillis, S. Doniach, and U. Spann. 1992. Small-angle x-ray scattering/diffraction system for studies of biological and other materials at the Stanford Synchrotron Radiation Laboratory. *Rev. Sci. Instrum.* 63:1736–1740.

Warner, L. E., M. J. Hilz, S. H. Appel, J. M. Killian, E. H. Kolodny, G. Karpati, S. Carpenter, G. V. Watters, C. Wheeler, D. Witt, A. Bodell, E. Nelis, C. Van Broeckhoven, and J. R. Lupski. 1996. Clinical phenotypes of different MPZ (P0) mutations may include Charcot-Marie-Tooth type 1B, Dejerine-Sottas, and congenital hypomyelination. *Neuron.* 17: 451–460.

Wells, C. A., R. A., Saavedra, H. Inouye, and D. A. Kirschner. 1993. Myelin P0-glycoprotein: predicted structure and interactions of extracellular domain. *J. Neurochem.* 61:1987–1995.

Worthington, C. R., and A. E. Blaurock. 1969. A structural analysis of nerve myelin. *Biophys. J.* 9:970–990.

Wu, C-F., and S-H. Chen. 1988. Small angle neutron and x-ray scattering studies of concentrated protein solutions. II. Cytochrome C. *Biopolymers.* 27:1065–1083.